Available online at http://scik.org

J. Math. Comput. Sci. 11 (2021), No. 5, 5458-5473

https://doi.org/10.28919/jmcs/6049

ISSN: 1927-5307

NUMERICAL STUDY OF MHD FLOW AND HEAT TRANSFER OF SUTTERBY NANO FLUID OVER A STRETCHING SURFACE WITH ACTIVATION ENERGY AND NIELD'S CONDITION

G. DHARMAIAH[1,*], K. S. BALAMURUGAN[2]

[1]School of Sciences, Career Point University, Kota, Rajasthan, India

[2]RVR&JC College of Engineering, Guntur, A.P., India

Abstract: The present study examines the numerical study regarding MHD Sutterby nano fluid flow over a stretching surface in the existence of activation energy. This investigation has been performed by using convective Nield boundary conditions. Effects of variable thermal conductivity, activation energy; nonlinear thermal radiation are considered. The governing nonlinear partial differential equations (PDEs) with convective boundary conditions are converted into the nonlinear ordinary differential equations (ODEs) with the help of similarity transformation, and then the resulting nonlinear ODEs are solved with MATLAB built inbvp4c solver. The computed results of velocity, temperature and concentration profiles are displayed by means of graphs. Skin-friction coefficient, Nusselt number and Sherwood number are computed and analyzed.

Keywords: Sutterby nanofluid; nonlinear analysis; activation energy; Nield's condition; MHD.

2010 AMS Subject Classification: 35F30, 49M30.

1. INTRODUCTION

The combined mass and heat transportation phenomenon driven by buoyancy force, due to variation of mass species and temperature is encountered in various chemical and process engineering applications, and therefore attention has been devoted by engineers in last decade.

*Corresponding author

E-mail address: raodg42@gmail.com

Received May 16, 2021

The impact of buoyancy-driven force on mass and heat transportation phenomenon is also momentous in the chemical processes where mass species differences of dis-similar species exist. Most interesting applications of this phenomenon include food processing, absorption, thermal wadding, diffusion of nutrition in tissues heat oil, heterogeneous catalysis in suspension cooling of nuclear reactors, and geothermal reservoir.

Nanofluids have gained immense importance in the present era in reference to its utility in controlling heat transfer within the system. In the present era, the cooling process is a much needed phenomenon in terms of applications to mitigate heating effects in computer chips, car engines etc. In past, the conventional liquids like water, oil, ethylene glycol were used for controlling the heat effects. Later on, a new technique containing solid-liquid mixture of nanoparticles and base liquid, named as nanofluid, was introduced by Choi[1]with lot of applications in biomedical, optical, electronics and ceramic industry. The heat absorption tendency of nanofluids is much higher than that of the traditional liquids. Research on nanoparticles by Das et al.,[2]Wang and Mujumdar [3],Usria et al., [4]and Murshed et al.[5] has concluded that mixing of nanoparticles with liquids enhances the thermal conductivity. Buongiorno [6] developed a model with Brownian motion and thermophoresis aspects.

Magnetohydrodynamics (MHD) is a study of magnetic effects in electrically conducting fluids.MHD has immense involvement in processes like earth magnetic field, solar wind, fusion, cooling of fission reactors, star formation, tumor therapy, X-ray radiation, plasmas, electrolytes etc. Dogonchi et al. [7] discussed the dissipative and MHD impacts in radiative convective nanofluid flow under diffusion theory. Dogonchi et al.[8] depicted the Darcian flow of radiative CuO-water nanofluid.

Recently, the activation energy has attained the interests of engineers, which was originally proposed by Arrhenius in 1889. This is known as base energy supplied to reactants in chemical processing for the conversion of products. The potential and kinetic energies are employed in molecules to stretch, twist, and break bonds. The idea of energy activation is more prominent in oil suspensions, industries of oil storage, hydrodynamics, and geothermal systems. Activation energy is defined as the minimum amount of energy owned by reacting specie to undergo an indicated reaction. The Arrhenius equation is usually of the form (Tencer et al. [9]):

$$K = B\left(\frac{T}{T_\infty}\right)^n \exp\left(\frac{-E_a}{\kappa T}\right) \tag{1}$$

Where K represents reaction rate constant, Ea is the activation energy, T the fluid temperature and B the pre-exceptional factor depicting an increase in the temperature with respect to increase in there action rate. Tointerpolate such energy activation effects, Maleque [10] studied the role of endothermic exothermic chemical reactions under energy activation. He noticed that the velocity profile increases by increasing the value of the Grashof number. Khan et al., [11] discussed the radiative nanofluid with energy activation. Rotating aspects in the flow of rate type material under energy activation were explored by Shafique et al., [12].

Motivated by the above-mentioned attempts, this paper focuses on the analysis of nano particles of heat transfer by incorporating hydro magnetic Sutterby fluid with activation energy with Nield's conditions. The literature survey witness that such analysis has not been performed yet. The governing nonlinear partial differential equations (PDEs) with convective boundary conditions are first converted into the nonlinear ordinary differential equations (ODEs) with the help of similarity transformation, and then the resulting nonlinear ODEs are solved with the help of MATLAB built inbvp4c solver. The computed results of velocity, temperature and concentration profiles are displayed by means of graphs. Skin-friction coefficient, Nusselt number and Sherwood number are computed and analyzed. The present analysis may be beneficial for academic research in the field of heat transfer and industry.

2. MATHEMATICAL MODELING

We consider the two-dimensional incompressible flow of Sutterby nano fluid past a stretching non porous sheet is analyzed. The Cartesian coordinate system is chosen for the flow analysis as shown in Fig. 1. Let u and v be the components of velocity in x and y directions respectively; the *x*-axis is taken along the stretching surface inthe direction of motion and the *y*-axis is perpendicular to it. Magnetic field B_0 is applied perpendicular to sheet. Reynolds number is considered very small so that the effect of induced magnetic field current can be neglected. The stretching surface velocity is $u(x) = ax$ along x axis. Temperature is regulated by the convective heating process described by the heat transfer coefficient h_f and the temperature of the hot fluid T_f.

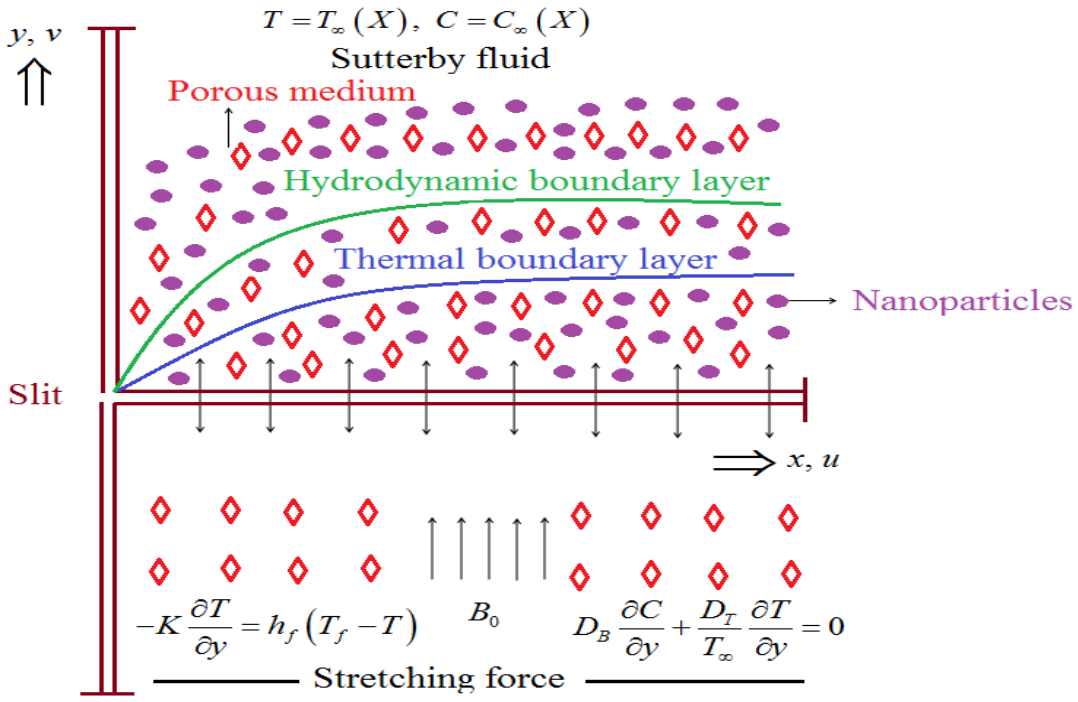

Fig 1. Engineering flow diagram

Under boundary layer assumption, the standard equations take the form (Azhar *et al* [13], Saif-ur-Rehman et al.[14], Sajid et. Al.,[15]):

$$\frac{\partial u}{\partial x}+\frac{\partial v}{\partial y}=0 \tag{2}$$

$$u\frac{\partial u}{\partial x}+v\frac{\partial u}{\partial y}=\frac{\mu_0}{\rho}\frac{\partial}{\partial y}\left[\frac{\partial u}{\partial y}+\frac{mB^2}{3}\left(\frac{\partial u}{\partial y}\right)^3\right]-\frac{\sigma_1 B_0^2(x)}{\rho}u \tag{3}$$

$$u\frac{\partial T}{\partial x}+v\frac{\partial T}{\partial y}=\left(\alpha_f+\frac{16\sigma_s T_\infty^3}{3k^*(\rho c)_f}\right)\frac{\partial^2 T}{\partial y^2}+\frac{(\rho C)_P}{(\rho C)_f}\left(D_B\frac{\partial C}{\partial y}\frac{\partial T}{\partial y}+\frac{D_T}{T_\infty}\left(\frac{\partial T}{\partial y}\right)^2\right) \tag{4}$$

$$u\frac{\partial C}{\partial x}+v\frac{\partial C}{\partial y}=D_B\frac{\partial^2 C}{\partial y^2}+\frac{D_T}{T_\infty}\frac{\partial^2 T}{\partial y^2}-k_c(C-C_\infty)\left(\frac{T}{T_\infty}\right)^n\exp\left(-\frac{E_a}{\kappa T}\right) \tag{5}$$

The corresponding boundary conditions are

$$u=u_w(x)=ax, v=0, -k\frac{\partial T}{\partial y}=h_f\left(T_f-T\right), D_B\frac{\partial C}{\partial y}+\frac{D_T}{T_\infty}\frac{\partial T}{\partial y}=0 \text{ at } y=0 \tag{6}$$

$$u\to 0, T\to T_\infty, C\to C_\infty \quad at \quad y\to\infty \tag{7}$$

In the concentration equation, the term $k_c\left(C-C_\infty\right)\left(\frac{T}{T_\infty}\right)^n \exp\left(-\frac{E_a}{\kappa T}\right)$ is the Arrhenius Expression and Kc - the reaction rate.

Where ρ - the fluid density, ν - the kinematic viscosity, $\left(\rho C\right)_f$ - the heat capacity of the fluid, $\left(\rho C\right)_p$ - the effective heat capacity of the nanoparticle material, k – the thermal conductivity, D_B - the Brownian diffusion coefficient, D_T - the thermophoretic diffusion coefficient, B - Sutterby fluid coefficient, σ_1 - represents electrical conductivity, B_0–the strength of constant magnetic field, T - the temperature of fluid, T_∞ - the free stream temperature, m - the power law index. Here m >0 , the shear thickening or dilatant fluid, m < 0 , the shear thinning or pseudo plastic fluid and form = 0, the fluid is simply a Newtonian fluid.

Let us introduce the following similarity variables:

$$u = axf'(\eta), v = -\sqrt{av}\, f(\eta), \eta = \sqrt{\frac{a}{\nu}}y, \theta(\eta) = \frac{T-T_\infty}{T_f-T_\infty}, \phi(\eta) = \frac{C-C_\infty}{C_w-C_\infty} \tag{8}$$

In view of the similarity transformation (8), eq. (2) is identically satisfied and eqs (3) – (7) are reduced to the followingnon-dimensional form:

$$f''' + \frac{m}{2}\mathrm{Re}\,De f''^2 + f(\eta)f''(\eta) - \left(f'(\eta)\right)^2 - Mf'(\eta) = 0 \tag{9}$$

$$\frac{1}{\mathrm{Pr}}\left(1+R\right)\theta'' + f\theta' + Nb\theta'\phi' + nt\theta'^2 = 0 \tag{10}$$

$$\phi'' + Scf\phi' + \frac{Nt}{Nb}\theta'' - Sc\sigma\left(1+\delta\theta\right)^n \exp\left(\frac{-E}{1+\delta\theta}\right)\phi = 0 \tag{11}$$

The associated boundary conditions are

$$f(0) = 0,\ f'(0) = 1, \theta'(0) = -\gamma\left(1-\theta(0)\right),\ Nb\theta'(0) + Nt\phi'(0) = 0 \quad at \quad \eta = 0 \tag{12}$$

$$f' = 0, \theta \to 0, \phi \to 0 \quad as \quad \eta \to \infty \tag{13}$$

where, prime represents the differentiation with respect to η, Re is Reynolds number, De is Deborah number, M is magnetic parameter, Nb is Brownian motion parameter, Pr is Prandtl number, Nt is Thermophoresis parameter, Le is Lewis number, σ is reaction rate constant, E is Activation Energy parameter, γ is Biot number, R is Thermal Radiation, n is order of the exponential of chemical reaction, δ is temperature difference.

Moreover, the definition of these physical dimensions less parameters is

$$\mathrm{Re}=\frac{ax^2}{\nu};\ E=\frac{E_a}{\kappa T_\infty};\ \delta=\frac{T_w-T_\infty}{T_\infty};\ \mathrm{Pr}=\frac{\nu}{\alpha};\ Le=\frac{\alpha}{D_B};\ \sigma=\frac{k_c}{c};\ \tau=\frac{\rho C_p}{\rho C_f};\ Nb=\frac{\tau D_B}{\nu}\left(C_w-C_\infty\right);$$

$$Nt=\frac{D_T}{T_\infty}\frac{\tau}{\nu}\left(T_w-T_\infty\right);\ De=B^2a^2;\ \gamma=\frac{h}{k}\sqrt{\frac{\nu}{c}} \tag{14}$$

The physical quantity namely skin friction coefficient for the present flow problem is transmuted below

$$C_f=\frac{\tau_w}{\rho_f u_e^2(x)}\Rightarrow -\mathrm{Re}_x^{1/2}C_f=f''(0)+\frac{m}{6}De\,\mathrm{Re}\left(f''(0)\right)^3 \tag{15}$$

The local Nusselt number is formulated as

$$Nu_x=\frac{xq_w}{k(T_w-T_\infty)} \tag{16}$$

Where the heat flux q_w is given by $q_w=-k\left(\frac{\partial T}{\partial y}\right)_{y=0}$ (17)

The dimensionless form of Nusselt number is given by

$$Nu_x\,\mathrm{Re}_x^{-\frac{1}{2}}=-(1+R)\theta'(0) \tag{18}$$

The local Sherwood number is formulated as

$$Sh_x=\frac{xC_w}{D_B(C_w-C_\infty)} \tag{19}$$

The dimensionless form of Sherwood t number is given by

$$\mathrm{Re}_x^{-1/2}\,Sh_x=-\phi'(0) \tag{20}$$

3. NUMERICAL SOLUTION

The highly nonlinear transformed system (9 - 11) with conditions (12, 13) is evaluated numerically using MATLAB built in bvp4c solver. Here we convert nonlinear equations into the system of first order ordinary differential equations, and then we solved it by using RK method of order 4. The iterative process will be terminated when the error involved is $< 10^{-5}$. The obtained computations are repeated by the iterative procedure so that results up to the 10^{-5} accuracies are obtained.

4. MAIN RESULTS

In this portion, influence of the eminent parameters is investigated on the velocity f', temperature θ and Sutterby nanofluid concentration ϕ. A detailed analysis of roles of distinct constraints is conferred. The velocity profile corresponding to the Deborah number exhibited in Fig. 2. It can be seen that the velocity profile enhances by increasing the value of Deborah number. Deborah number is actually determines the difference amongst solids and fluids. On account of smaller Deborah number the material responds like fluid however inverse on account of large value of Deborah number where material acts like solids. The contribution of power law index m is depicted in Figure 3. As m increases, $f'(\eta)$ also increases.

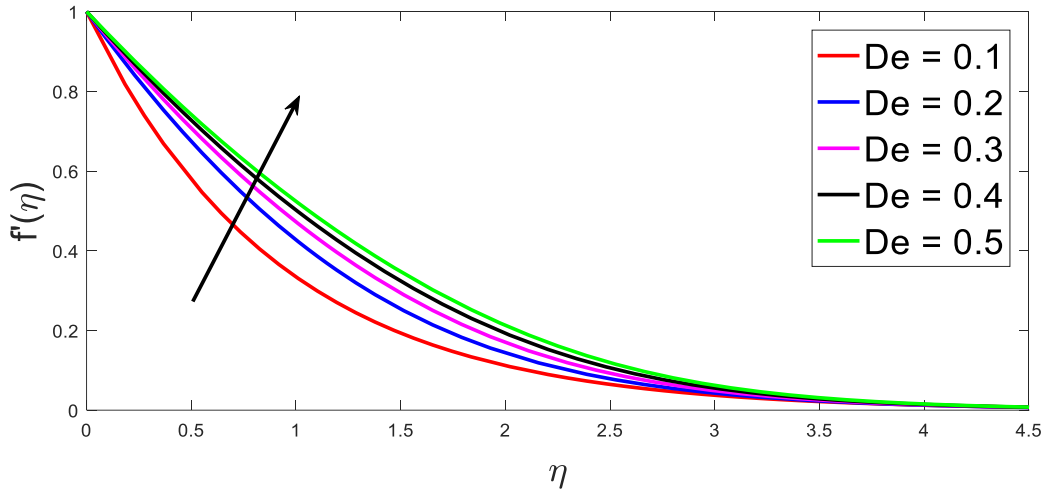

Fig 2. Variation of De on Velocity.

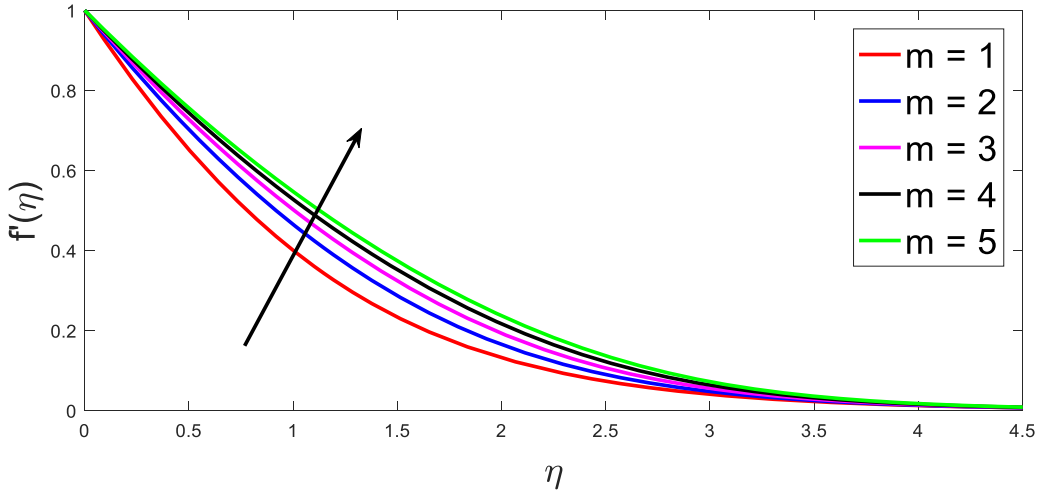

Fig 3. Variation of m on Velocity.

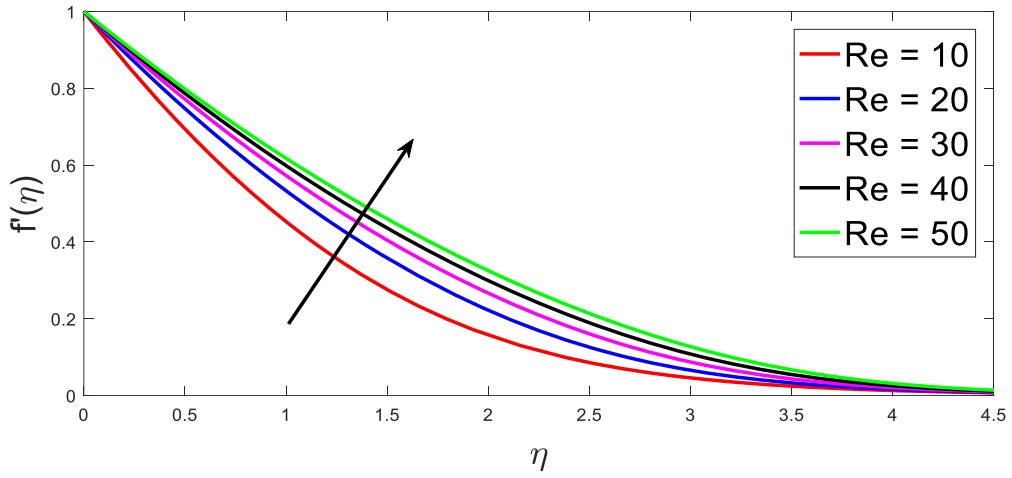

Fig 4. Variation of Re on Velocity.

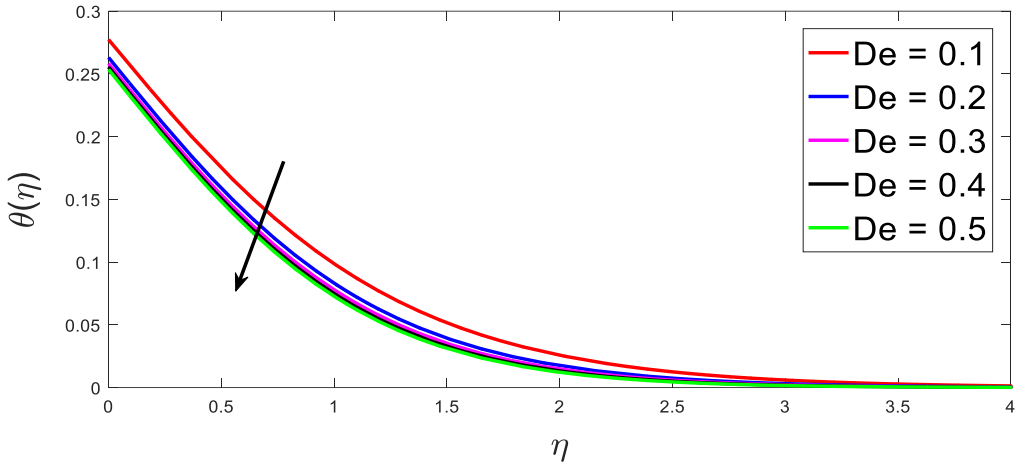

Fig 5. Variation of De on Temperature.

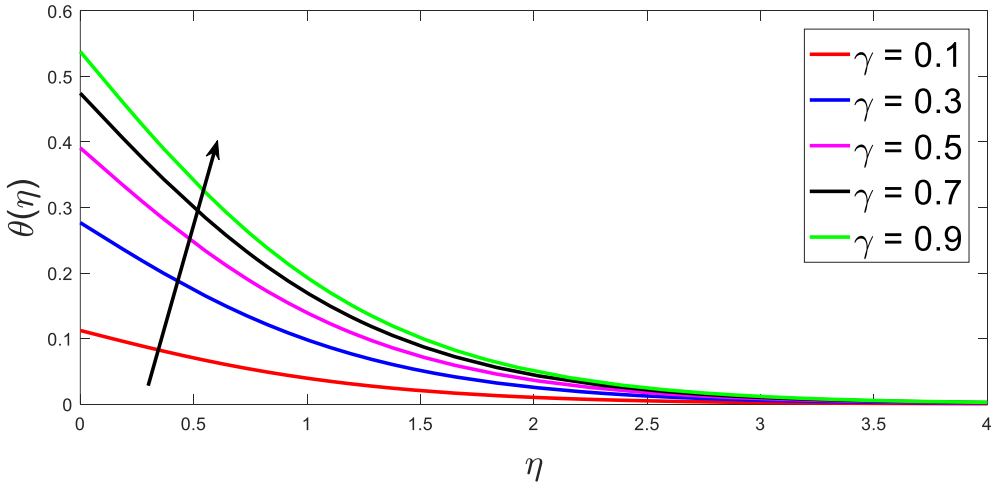

Fig 6. Variation of γ on Temperature.

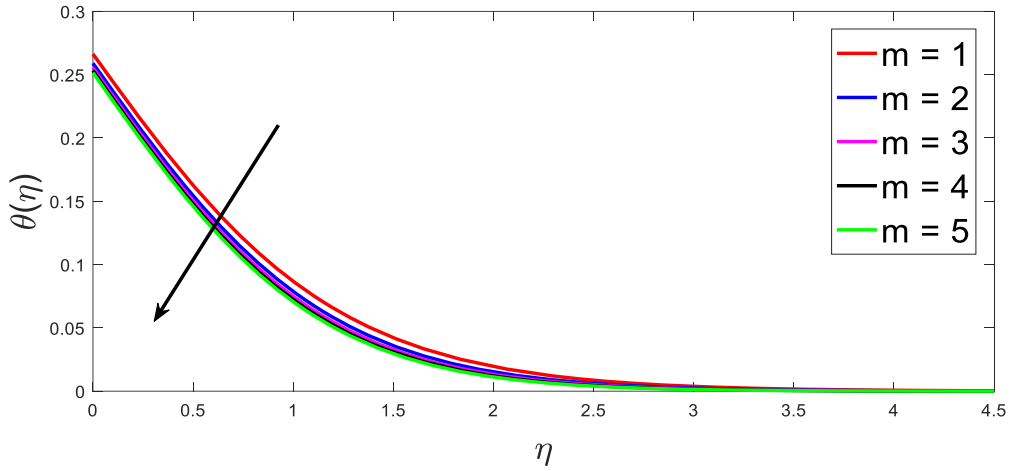

Fig 7. Variation of m on Temperature.

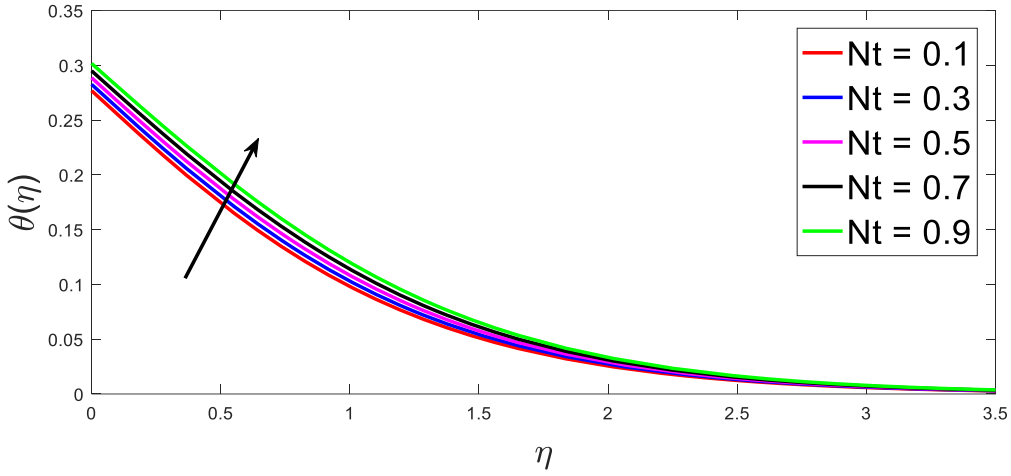

Fig 8. Variation of Nt on Temperature.

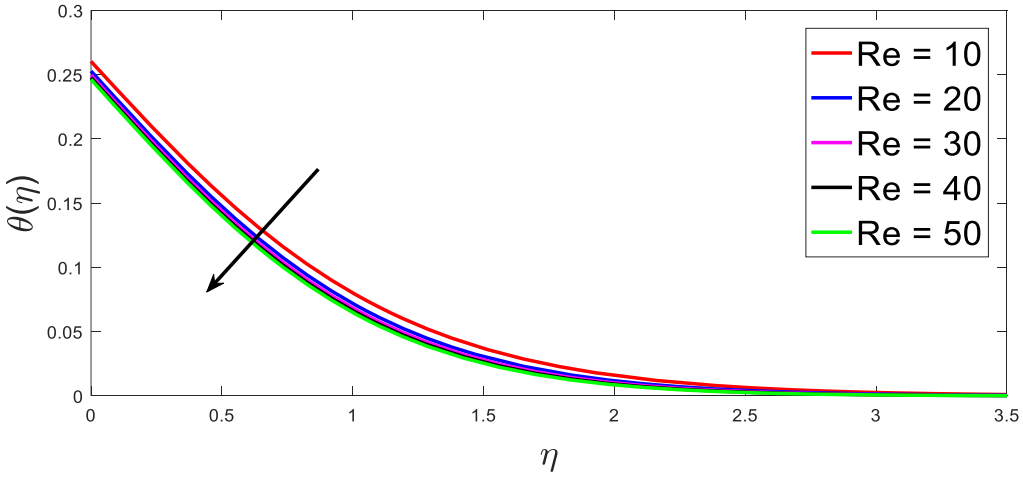

Fig 9. Variation of Re on Temperature.

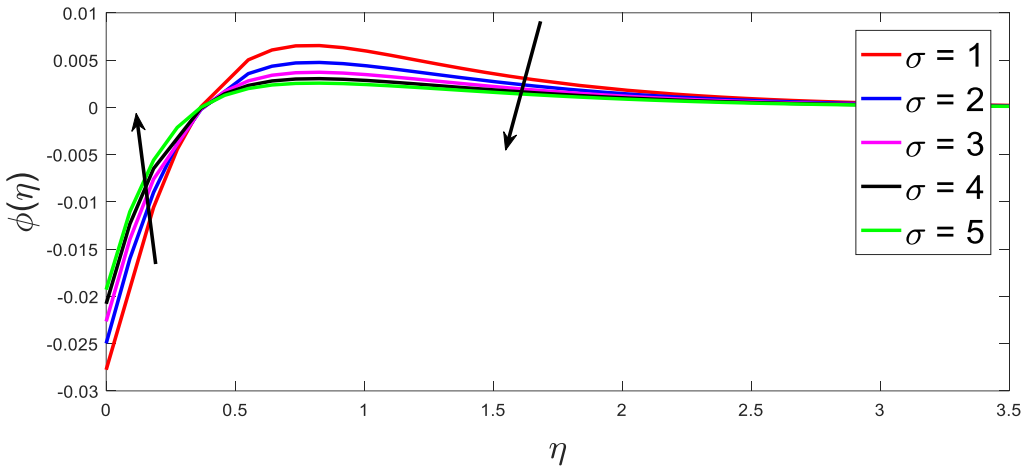

Fig 10. Variation of σ on Concentration.

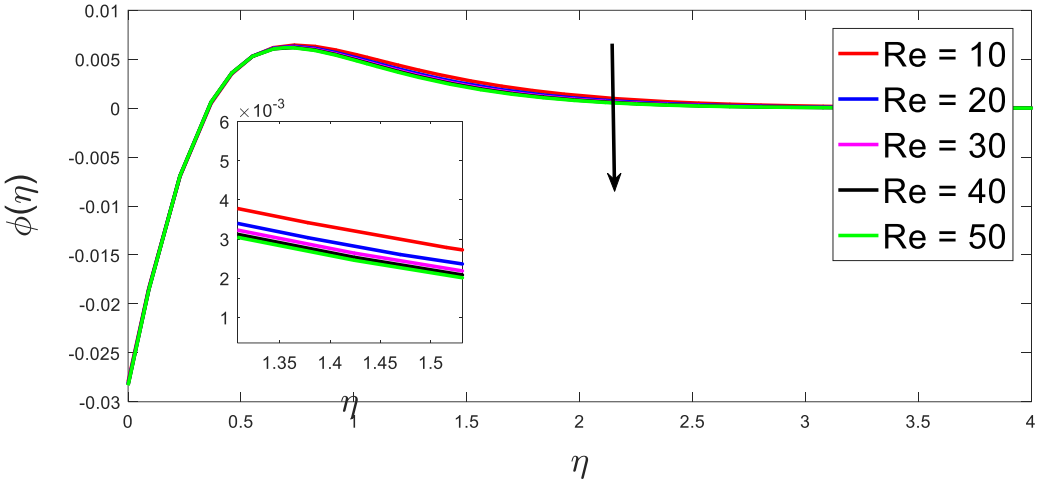

Fig 11. Variation of Re on Concentration.

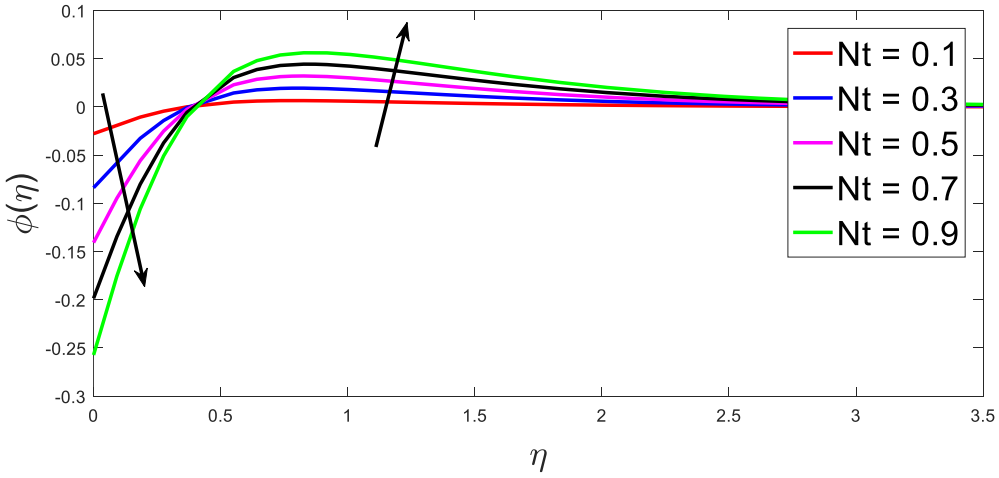

Fig 12. Variation of Nt on Concentration.

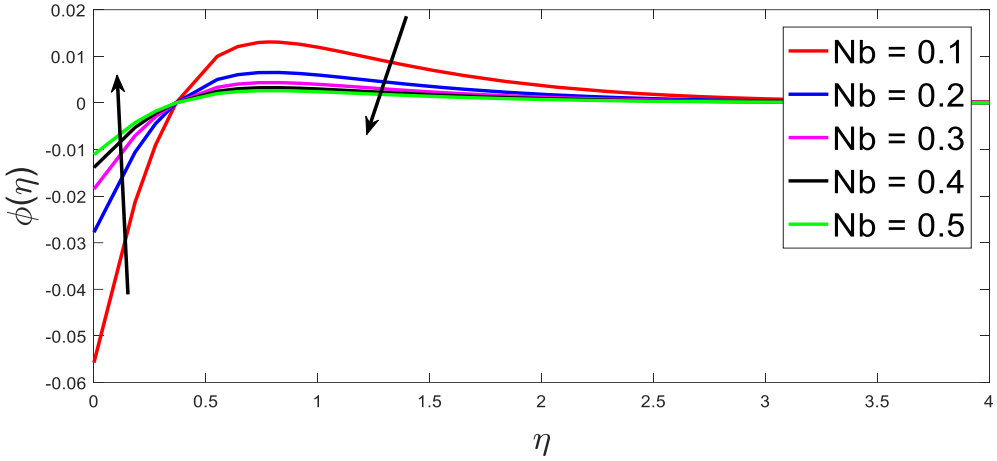

Fig 13. Variation of Nb on Concentration.

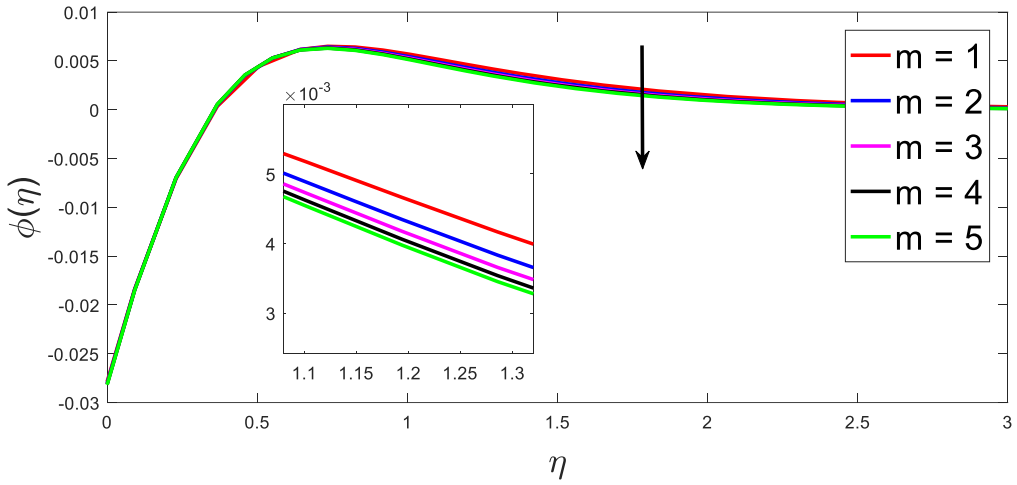

Fig 14. Variation of m on Concentration.

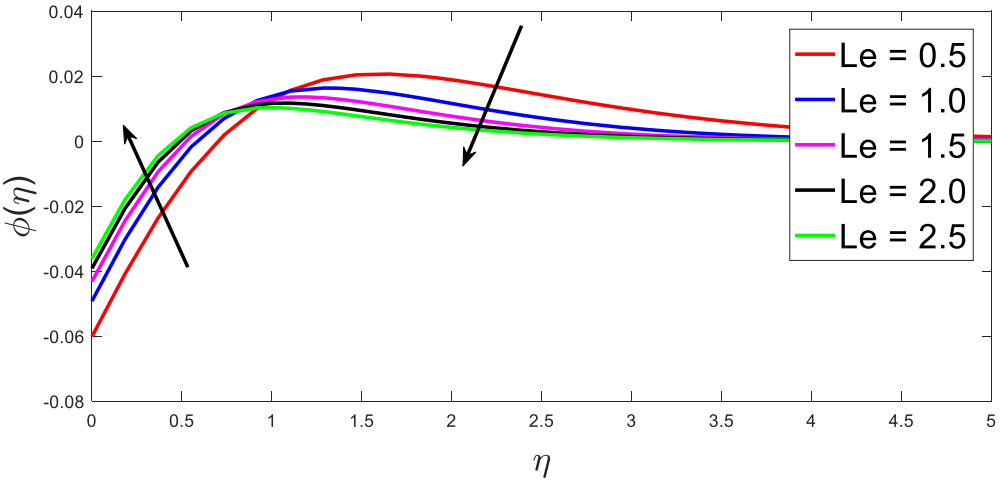

Fig 15. Variation of Le on Concentration.

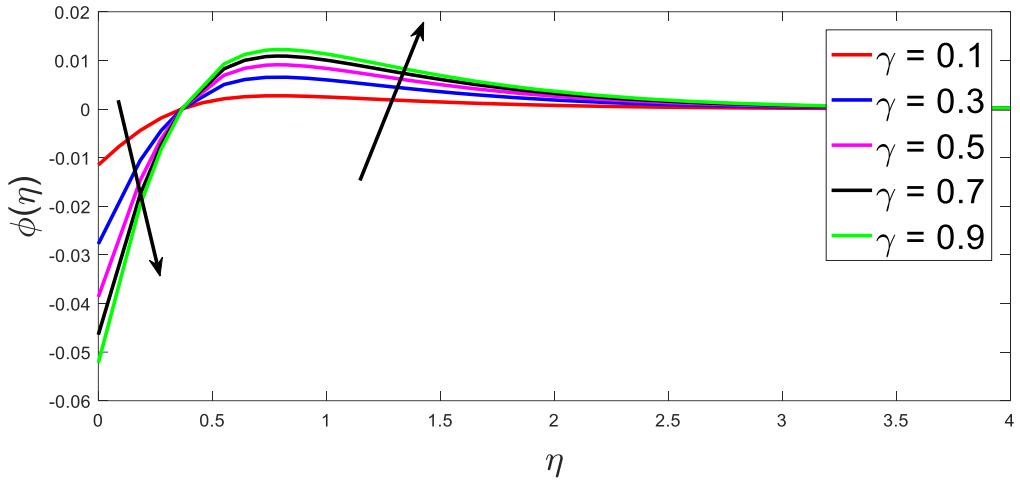

Fig 16. Variation of γ on Concentration.

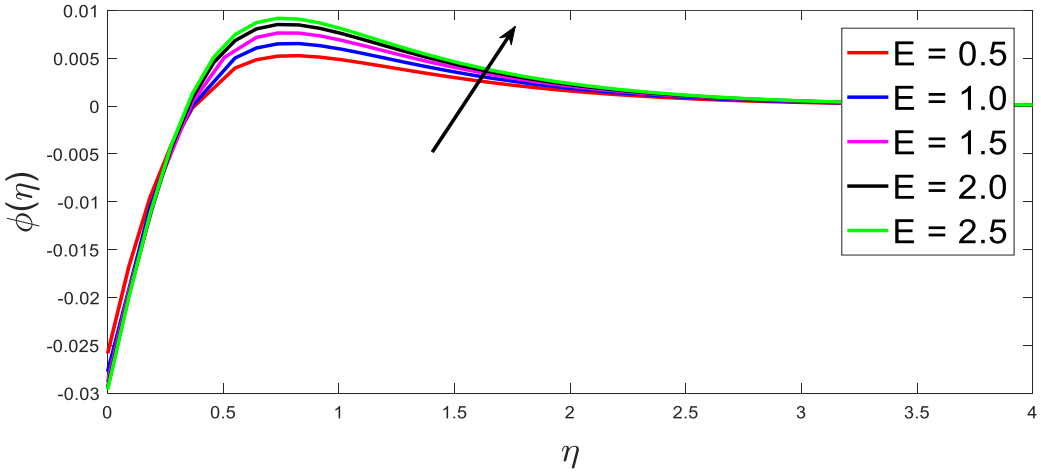

Fig 17. Variation of E on Concentration.

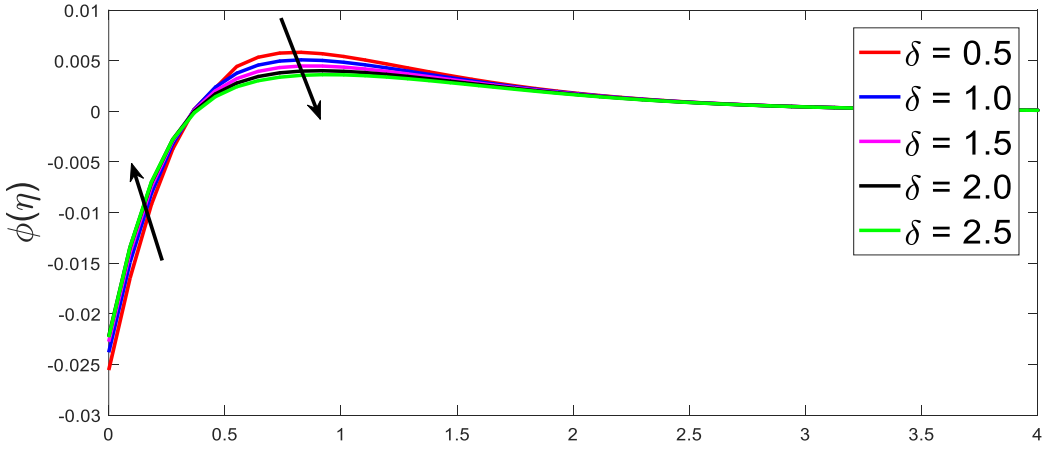

Fig 18. Variation of δ on Concentration.

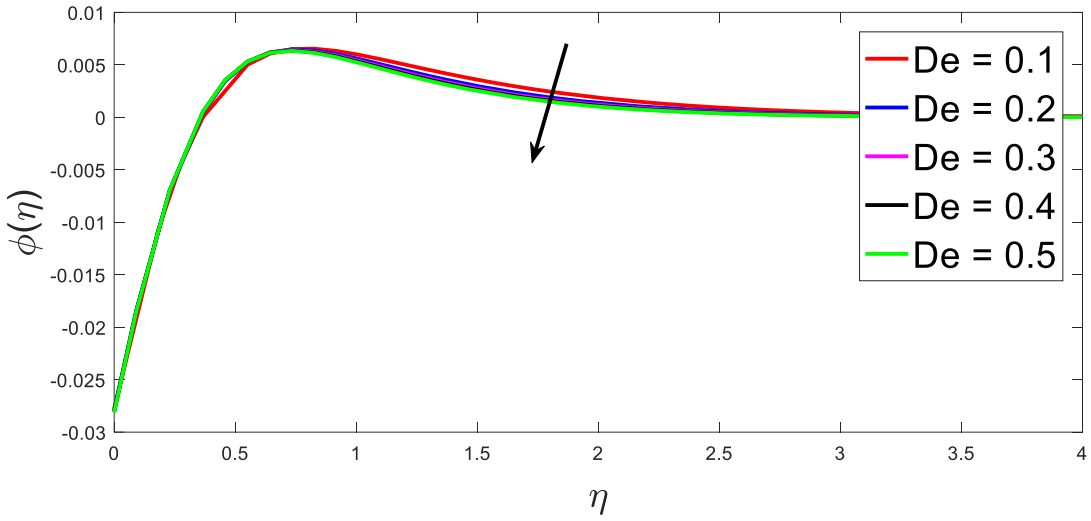

Fig 19. Variation of De on Concentration.

A figure 4 displays the behavior of Reynolds number. For high Reynolds number, viscous forces increase and as a result fluid velocity increase. Figure 5 shows the effect of Deborah number De on the temperature profile. From this figure it can be seen that the thermal boundary layer thickness decreases with the increase in Deborah number. An increase in De plays a role in increasing the viscous forces and elastic forces, respectively, which leads to an enhancement in viscous boundary layer, affecting the thermal boundary layer by reducing it. Fig. 6 illustrates that temperature is increasing function of thermal Biot number γ. As expected for γ convective heating at surface increases due to which transfer of heat to fluid increases which results enhancement in fluid temperature and thickness of the thermal boundary layer. Figure 7 indicates the contribution of power-law index m on θ (η). Prominent temperature is observed for shear thinning fluids retards. The behavior of the thermophoresis parameter has been discussed in Fig. 8, where a rise in the thermophoresis parameter Nt seems to rise the fluid temperature. The reason behind the rise in temperature is an increment in the nanoparticles. It is observed that the nanoparticles present close to the hot boundary have been shifted towards the cold fluid in the presence of the thermophoretic force, that's why the thermal boundary layer becomes thicker. The behavior of the Reynolds number has been discussed in Fig. 9, where a rise in the Reynolds number seems to retards the fluid temperature. Fig. 10 indicates the behavior of the nanoparticle concentration for the reaction rate constant. It is clear that an increase in the chemical reaction

parameter σ results in a increment in [0, 0.5] and decrement in [0.5, 3.5] on nanoparticle concentration. When we upgrade the value of reaction rate parameter σ brings about an augmentation in the term $\sigma(1+\delta\theta)^n \exp\left(\frac{-E}{1+\delta\theta}\right)$. This inevitably leads to a destructive chemical reaction. Due to this concentration profile rises. The influence of Reynolds number on concentration is studied. It is shown that concentration is a decreasing function of Re. An increase in the values of the thermophoresis parameter results an increment in concentration profiles. When the thermophoresis parameter increases, we expect a severe diffusion of nanoparticles in the base fluid. It causes the concentration boundary layer to rises as shown in Fig. 12. As Nt decreases in [0, 0.5] and increases in [0.5, 3.5]. Species concentration increases in [0, 0.5] and decreases [0.5, 4] with an increase in Brownian motion from figure 13. Figure 14 elucidates that the concentration decreases with an increase power law index parameter. Fig. 15 exhibits the variation of the nanoparticle concentration profile subject to the Lewis number. It is analyzed that by increasing the value of the Lewis number, it is enhances in [0, 0.5] and reduces [0.5, 4] in the concentration is observed. The plot of the Biot number γ against the concentration profile is displayed in Fig. 16. When the Biot number increases, the value of the concentration profile and the thickness of concentration layer reduces in [0, 0.5] and enhances [0.5, 4] also increase. Fig. 17 explores the behavior of the activation energy against the nanoparticle concentration profile. The Arrhenius function decays by increasing the value of the activation energy, which results in the promotion of the generative chemical reaction causing an augmentation in the concentration profile. Within the occurrence of low temperature and higher activation energy leads to a smaller reaction rate constant which slow down the chemical reaction, in this manner concentration of solute rises. The effect of δ on the concentration is plotted in figure 18. On account of high temperature and low concentration leads to larger reaction rate constant σ, which speed up the chemical reaction, concentration of solute enhances in [0, 0.5] and declines in [0.5, 4]. Impact of Deborah number against concentration profile is portrayed in Fig. 19. It is seen that, as De increases, concentration retards.

Table 1. Skin friction, Rate of Heat transfer and Rate of mass transfer for various values

De	Re	M	m	C_f	Nu	Sh
1				1.1238	0.2608	0.1087
2				1.1479	0.2613	0.1089
3				1.1693	0.2617	0.1091
4				1.1886	0.2621	0.1093
	10			1.1693	0.2617	0.1091
	20			1.1827	0.2628	0.1095
	30			1.2662	0.2635	0.1098
	40			1.3035	0.2641	0.1100
		1		1.4323	0.2540	0.1058
		2		1.7637	0.2475	0.1031
		3		2.0471	0.2419	0.1008
		4		2.3000	0.2370	0.0988
			0.5	1.1045	0.2604	0.1083
			1.0	1.1131	0.2605	0.1085
			1.5	1.1212	0.2607	0.1087
			2.0	1.1289	0.2609	0.1089

Table 1 represents the effect of dimensionless parameters De, Re, M and m on numerical values of skin friction, rate of heat flux and rate of mass flux. The increasing values of all these parameters enhance the coefficient of skin-friction. It is observed that the values of Nu and Sh decreases as M increases and m, Re, and De increase the contribution of Nu and Sh.

5. CONCLUSIONS

In this study, the characterization of Sutterby nanoparticles in flow induced by the stretching surface is reported. Results on the behavior of several physical parameters, eminent findings are enlisted as: The presence of nanoparticles improves the thermal conductivity and temperature profile effectively. In general, the radiation phenomenon can play an essential role in the enhancement of heat transfer. Brownian motion and thermophoresis parameters result in increment of fluid temperature. Brownian parameter decreases the fluid concentration whereas concentration grows by the thermophresis parameter. Coefficient of skin friction reinforce for all significant parameters.

CONFLICT OF INTERESTS

The author(s) declare that there is no conflict of interests.

REFERENCES

[1] S. U. S. Choi, Enhancing thermal conductivity of fluids with nanoparticles, Amer. Soc. Mech. Eng. 231 (1995), 99–105.

[2] S. K. Das, S. U. S. Choi, W. Yu, T. Pradeep, Nanofluids: Science and Technology, Wiley, New Jersey, 2007.

[3] X. Wang, A. S. Mujumdar, A review model of nanofluids: Theoretical and numerical investigations, Brazil. J. Chem. Eng. 55 (2008), 613–630.

[4] N. A. Usria, W. H. Azmi, R. Mamat, K. A. Hamid, and G. Najafi, Thermal conductivity enhancement of Al_2O_3 nanofluid in ethylene glycol and water mixture, Energy Procedia, 79 (2015), 397–402.

[5] S. M. S. Murshed, K. C. Leong, C. Yang, Investigations of thermal conductivity and viscosity of nanofluids, Int. J. Therm. Sci. 47 (2008), 560–568.

[6] J. Buongiorno, Convective transport in nanofluids, ASME J. Heat Transfer, 128 (2006), 240–250.

[7] A.S.Dogonchi, D.D.Ganji, Effect of Cattaneo–Christov heat flux on buoyancy MHD nanofluid flow and heat transfer over a stretching sheet in the presence of Joule heating and thermal radiation impacts, Indian J. Phys. 92 (2018), 757–766.

[8] A.S.Dogonchi, M. Waqas, S.M.Seyyedi, M. Hashemi-Tilehnoee, D.D.Ganji, Numerical simulation for thermal radiation and porous medium characteristics in flow of CuO-H_2O nanofluid, J. Brazil. Soc. Mech. Sci. Eng. 41 (2019), 249.

[9] M. Tencer, J. S. Moss, T. Zapach, Arrhenius average temperature: The effective temperature for non-fatigue wearoutand long term reliability in variable thermal conditions and climates, IEEE Trans. Components Packag. Technol. 27 (2007), 602–607.

[10] K.A. Maleque, Effects of exothermic/endothermic chemical reactions with Arrhenius activation energy on MHD free convection and mass transfer flow in presence of thermal radiation, J. Thermodyn. 2013 (2013), Article ID 692516.

[11] M.I.Khan, T.Hayat, M.I.Khan, A.Alsaedi, Activation energy impact in nonlinear radiative stagnation point flow of Cross nanofluid, Int. J. Commun. Heat Mass Transf. 91 (2018), 216-224.

[12] Z. Shafique, M. Mustafa, A. Mushtaq, Boundary layer flow of Maxwell fluid in rotating frame with binary chemical reaction and activation energy, Results Phys. 6 (2016), 627-633.

[13] E. Azhar, Z. Iqbal, E. N. Maraj, Impact of Entropy Generation on Stagnation-Point Flow of Sutterby Nanofluid: A Numerical Analysis, Z. Naturforsch. A 71 (2016), 837-848.

[14] B. Saif-ur-Rehmana, NazirA.Mir, M. Farooq, M. Rizwan, F. Ahmad, S. Ahmad, B. Ahmad, Analysis of thermally stratified flow of Sutterby nanofluid with zero mass flux condition, J. Mater. Res. Technol. 9 (2020), 1631–1639.

[15] T. Sajid, M. Sagheer, S. Hussain, M. Bilal, Darcy-Forchheimer flow of Maxwell nanofluid flow with nonlinear thermal radiation and activation energy, AIP Adv. 8 (2018), 035102.